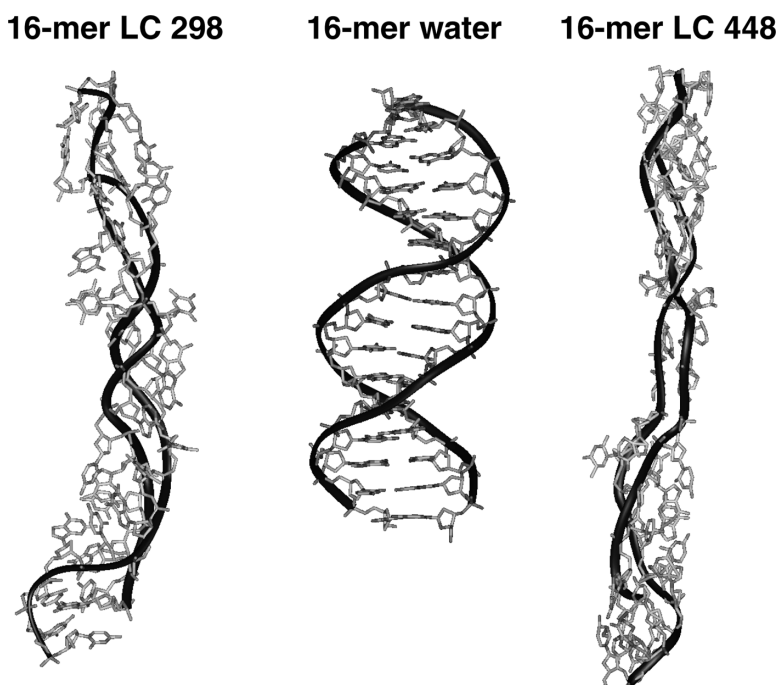


The Structure and Dynamics of DNA in the Gas Phase

Manuel Rueda, Susana G. Kalko, F. Javier Luque, and Modesto Orozco

J. Am. Chem. Soc., **2003**, 125 (26), 8007-8014 • DOI: 10.1021/ja0300564 • Publication Date (Web): 07 June 2003

Downloaded from <http://pubs.acs.org> on March 29, 2009



More About This Article

Additional resources and features associated with this article are available within the HTML version:

- Supporting Information
- Links to the 6 articles that cite this article, as of the time of this article download
- Access to high resolution figures
- Links to articles and content related to this article
- Copyright permission to reproduce figures and/or text from this article

[View the Full Text HTML](#)



The Structure and Dynamics of DNA in the Gas Phase

Manuel Rueda,[†] Susana G. Kalko,[†] F. Javier Luque,^{*,‡} and Modesto Orozco^{*,†,§}

Contribution from the Institut de Recerca Biomèdica, Parc Científic de Barcelona, Josep Samitier 1-5, Barcelona 08028, Spain, Departament de Fisicoquímica, Facultat de Farmàcia, Universitat de Barcelona, Avda Diagonal 643, Barcelona 08028, Spain, and Departament de Bioquímica i Biologia Molecular, Facultat de Química, Universitat de Barcelona, Martí i Franquès 1, Barcelona 08028, Spain

Received January 28, 2003; Revised Manuscript Received April 25, 2003; E-mail: modesto@mmb.pcb.ub.es; javier@far1.far.ub.es

Abstract: The impact of the transfer from water to the vacuum in the duplex DNA has been explored by using long molecular dynamic simulations. In opposition to chemical intuition, it is found that vaporization of DNA, even at high temperatures, does not lead to a total disruption of the double helix. Rather, the DNA duplex preserves gross structural, energetic, and dynamic features of the conformation of the double helix in aqueous solution. Thus, the two strands remain bound, the global structure has a slight helicity, and the total number of DNA–DNA interactions is not dramatically different from that found in solution. The results provide detailed structural and dynamic information useful to complement current mass spectroscopy studies of DNA structures.

Introduction

The right-handed double stranded helix of the DNA is very stable in aqueous solution,¹ and even small (~10 base pair) duplexes maintain their structure at moderately high temperatures.^{2,3} The stability of the DNA duplex stems from a subtle balance of different energy contributions. Particularly, the destabilizing repulsion between charged phosphates is compensated by stacking and hydrogen bond (H-bond) interactions between the bases and by the screening effect of the water and the ionic atmosphere. In fact, hydration is crucial for the stability of the duplex, since the change from aqueous to more apolar solvents leads to important conformational transitions or even to the disruption of the double helix.^{4–6} Accordingly, the transfer of DNA from water to the gas phase should presumably disrupt the double helix due to the tremendous unscreened repulsion between phosphate groups. However, electrospray experiments^{7–12} have recently challenged this latter assumption, since the DNA seems to adopt a duplex structure

somehow similar to that found in aqueous solution. Moreover, the same experiment suggests that the DNA can form structure-specific noncovalent interactions with small drugs,^{7–11} maintaining a nonnegligible amount of H-bonding between the two strands.¹² In summary, experimental data suggest a certain conservation in the structure of DNA upon transfer to the gas phase.

Because the experimental determination of the detailed structure of the DNA in vacuo is not feasible at present, molecular simulation techniques are the only suitable approach to explore in detail the structural, energetic, and dynamic properties of the DNA duplex in the gas phase. This paper reports the results of very extended molecular dynamics (MD) simulations carried out to examine the changes in the DNA induced upon vaporization. To our knowledge, this study provides the first direct evidence that a distorted double helix can exist in the gas phase, at least in the submicrosecond time scale.

Methods

MD simulations of the DNA in vacuo and control simulations in aqueous solutions were performed for the Dickerson dodecamer d(CGCGAATTCGCG) and a 16-mer duplex containing the same central sequence, d(CGCGCGAATTCGCGCG). The starting structures for the 12-mer and 16-mer duplexes were taken from crystal¹³ and fiber diffraction¹⁴ data, respectively. For the shortest sequence, an NMR structure is also available,¹⁵ which allows us to compare our simulations with both crystal and NMR data.

Simulations in Water. The starting structures of the duplexes were immersed in a polyhedral box containing 2068 and 3524 water

[†] Institut de Recerca Biomèdica.

[‡] Facultat de Farmàcia, Universitat de Barcelona.

[§] Facultat de Química, Universitat de Barcelona.

- (1) Watson, J. D.; Crick, F. H. C. 1953 *Nature* **1953**, *171*, 1303.
- (2) Blackburn, G. M.; Gait, M. J. *Nucleic Acids in Chemistry and Biology*; IRL Press: Oxford, 1990; pp 17–70.
- (3) Bloomfield, V. A.; Crothers, D. M.; Tinoco, I. *Nucleic Acids. Structure, Properties and Function*; University Science Books: Sausalito, CA, 2000; pp 165–217.
- (4) Herkovits, T. T.; Hattington, J. P. *Biochemistry* **1972**, *11*, 4800.
- (5) Levine, L.; Gordon, J. A.; Jencks, W. P. *Biochemistry* **1963**, *2*, 168.
- (6) Turner, D. H. In *Nucleic Acids. Structure, Properties and Functions*; Bloomfield, V. A., Crothers, D. M., Tinoco, I., Eds.; University Science Books: Sausalito, CA, 2000; pp 308–310.
- (7) Gale, D. C.; Smith, R. D. *J. Am. Soc. Mass. Spectrom.* **1995**, *6*, 1154.
- (8) Hofstadler, S. A.; Griffey, R. H. *Chem. Rev.* **2001**, *101*, 377.
- (9) Gabelica, V.; De Pauw, E.; Rosu, F. *J. Mass. Spectrom.* **1999**, *34*, 1328.
- (10) Wan, K. X.; Shibue, T.; Gro, M. L. *J. Am. Chem. Soc.* **2000**, *122*, 300.
- (11) Reyzer, M. L.; Brodbelt, J. S.; Kerwin, S. M.; Kuman, D. *Nucl. Acid Res.* **2001**, *29*, 103.
- (12) Schnier, P. D.; Klassen, J. S.; Strittmatter, E. F.; Williams, E. R. *J. Am. Chem. Soc.* **1998**, *120*, 9605.

- (13) Drew, H. R.; et al. *Proc. Natl. Acad. Sci. U.S.A.* **1981**, *78*, 2179.
- (14) Arnott, S.; Bond, P. J.; Selsing, E.; Smith, P. J. C. *Nucl. Acid Res.* **1976**, *3*, 2459.
- (15) Kuszewski, J.; Schwieters, C.; Clore, G. M. *J. Am. Chem. Soc.* **2001**, *123*, 9303.

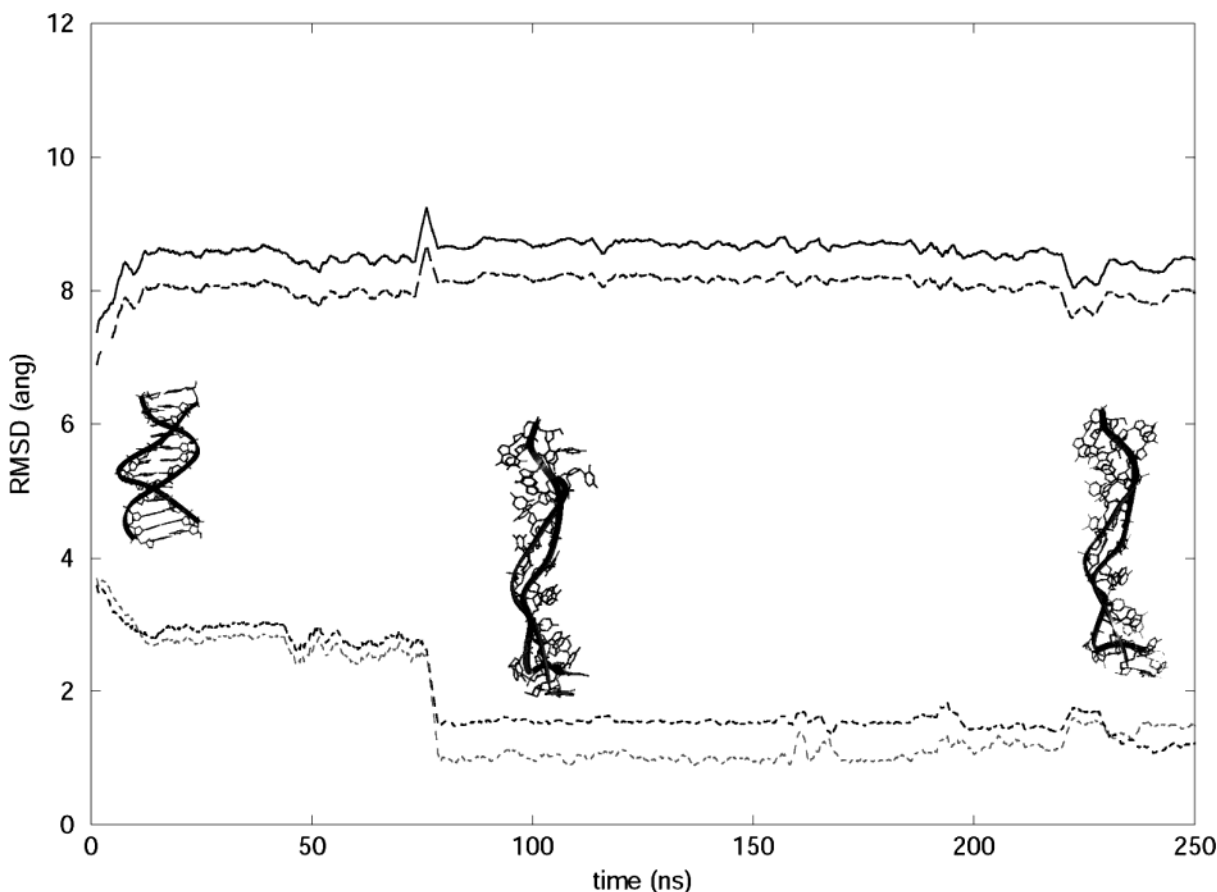


Figure 1. RMSD (Å) between the 12-mer oligonucleotide (simulation at 298 K with the LC charge state) in the gas phase and several reference structures during an extended 250 ns trajectory: continuous crystal structure, dashed line NMR structure); MD-averaged structure, dotted line (90–100 ns), light-dotted line 240–250 ns).

molecules and neutralized by adding 22 and 30 sodium counterions placed around the phosphate groups. They were subsequently optimized and equilibrated using our standard multistep protocol.¹⁶ Periodic boundary conditions, the PME method,¹⁷ SHAKE,¹⁸ and a 2 fs time step were used. Simulations were performed using AMBER-99¹⁹ and TIP3P²⁰ force fields and the AMBER 5.1 suite of programs.²¹

Simulations in Vacuo. The snapshots collected at 5 ns in the MD simulations in water were used as starting structures after removal of water molecules and counterions. RESP(HF/6-31G(d)) charges were derived for neutral phosphates.²² Because charges adapted to represent the DNA in aqueous solution might not be suitable for the in vacuo calculation, additional MD simulations where the charges of nucleobases were scaled by a factor of 0.8 were performed. However, pilot calculations showed that these subtle changes in force-field parameters have little influence in the conformational transition of the DNA duplex.

The torsional barriers for the P(O)–O(H) bond were set to zero, and the bending constant for the H–O–P angle was increased to 250 kcal mol⁻¹ rad² to avoid discontinuities in the energy profile. The rest of parameters were taken from the standard AMBER-99 force field. No cutoff was used for nonbonded interactions. SHAKE and 1 fs step

were also used. The resulting structures were equilibrated at 298 K for 100 ps starting from the velocities of the MD simulation in water. After equilibration, 100 ns MD simulations (one of the trajectories was extended to 250 ns; see Figure 1) were performed at constant temperature (298 K). The structures obtained after 1 ns were used as starting points for additional MD simulations at 448 K after heating from 298 to 448 K in 100 ps.

A delicate decision for MD simulations in the gas phase was the assignment of the charge state of the duplex, since control simulations of fully charged and fully neutral duplexes yielded completely unfolded structures and coil conformations showing no helicity, respectively. According to electrospray experiments,^{7,9,10} a net charge of –6 and –8 was assigned to the 12-mer and 16-mer duplexes, respectively. Since there is no information about the location of these charges in the duplex, two neutralization protocols were considered. First, negative charges were assigned to the set of 6/8 phosphates that minimize the distance function ζ (eq 1, where the sum extends for a set of 6/8 phosphates),

$$\zeta = \sum_{ij} \frac{1}{d_{ij}} \quad (1)$$

while the rest of the phosphates were neutralized by adding a proton to the O₁P atom. Second, the total net charge was equally distributed along all the phosphates by appropriate scaling of their charges (eq 2, where i stands for the atoms in the phosphate unit, α is the net charge of the DNA duplex (–6 or –8), and β is the total number of phosphates in the duplex).

$$Q_i^{\text{scaled}} = \frac{\alpha}{-\beta} Q_i \quad (2)$$

(16) Harris, S. A.; Gavathiotis, E.; Searle, M. S.; Orozco, M.; Laughton, C. A. *J. Am. Chem. Soc.* **2001**, *123*, 12658.

(17) Darden, T. A.; York, D.; Pedersen, L. *J. Chem. Phys.* **1993**, *98*, 10089.

(18) Ryckaert, J. P.; Ciccotti, G.; Berendsen, H. J. C. *J. Comput. Phys.* **1977**, *23*, 327.

(19) Cheatham, T. E.; Cieplak, P.; Kollman, P. A. *J. Biomol. Struct. Dyn.* **1999**, *16*, 8458.

(20) Jorgensen, W. L.; Chandrasekhar, J.; Madura, J. D.; Impey, R. W.; Klein, M. L. *J. Chem. Phys.* **1983**, *79*, 926.

(21) Case, D. A.; et al. AMBER 5, University of California, San Francisco, 1997.

(22) Bayly, C. E.; Cieplak, P.; Cornell, W. D.; Kollman, P. A. *J. Phys. Chem.* **1993**, *97*, 10269.

These neutralization protocols, therefore, represent two limit scenarios corresponding to duplexes with fully localized (LC) and fully distributed (DC) charges. For each duplex and charge neutralization protocol, MD simulations were performed at 298 and 448 K, with this latter temperature being typically used in electrospray experiments.^{9,10} Thus, a total set of 8 independent trajectories (of at least 0.1 μ s each) covering around 1 μ s of unrestricted MD simulation in vacuo were run. This wide set of simulations allowed us to obtain a quite complete picture of the behavior of DNA in the gas phase.

Analysis of the Trajectories. Trajectories were analyzed to DNAs from structural, energetic, and dynamic points of view. In house programs were used to determine geometric and energetic properties of the different structures. The dynamic characteristics of the structures were analyzed using Principal Component Analysis (PCA) technique. Accordingly, covariance matrices were built up (excluding the HO1-(P) atoms in LC simulations), removing the nucleotides at the extremes of the duplexes to avoid end-effects. These covariance matrices were then diagonalized to derive the eigenvalues and eigenvectors defining the essential dynamic of the DNAs. In all cases the trajectories were projected along the first modes of motion to discard the existence of Fourier-shaped profiles, which would indicate the existence of massive random movements in the DNA.²³

The similarity in the dynamic behavior of the duplexes in two trajectories was analyzed by comparing the frequencies, which measure the extent of the conformational motions occurring along the trajectory, and the associated eigenvectors, which define the nature of the conformational motions. The similarity between eigenvectors was quantified from the absolute (γ) and relative (κ) similarity indexes shown in eqs 3 and 4,

$$\gamma_{AB} = \frac{1}{n} \sum_{i=1}^n \sum_{j=1}^n (\nu_i^A \cdot \nu_j^B)^2 \quad (3)$$

$$\kappa_{AB} = 2 \frac{\gamma_{AB}}{\gamma_{AA}^T + \gamma_{BB}^T} \quad (4)$$

where ν are principal component (3xN dimensional, for N being number of atoms) vectors, A and B stand for two different trajectories of equal length (with trajectories defined along a common reference system), and the self-similarity indexes γ_{AA}^T and γ_{BB}^T are obtained by using eq 3 for the same trajectories using two nonoverlapping portions of equal time length.

Entropies of the different oligonucleotides were determined using 3 to 10 ns samplings (see Results and Discussion) using the quasiharmonic Schlitter method.²⁴ Entropy values for infinite simulation time were derived from 10 ns trajectories using the extrapolation technique developed by Harris et al.²⁵

Nucleobase–nucleobase interaction maps were computed to determine the energetic of nucleobase–nucleobase contacts. They were computed using the standard AMBER-99 force field from the snapshots collected during the trajectories. Nucleobases were capped at the C1' atom by a CH₃ group to obtain neutral groups. This allows reduction in the noise of the averages.

Results and Discussion

Unrestrained MD simulations of 15 (12-mer) and 6 (16-mer) ns at constant pressure and temperature (1 atm, 298 K) in water yield stable structures, very close to the experimental ones, as noted in the RMSd values (see Figure 2 and Table 1). H-bonds are fully preserved along the entire trajectory. Moreover, the phosphate contact maps and helical parameters (data not shown),

Table 1. Average Root Mean Square Deviations (rmsd) between the Different Trajectories and Reference Structures Taken from Fiber Diffraction, X-ray (PDB entry 1BNA), and NMR (PDB entry 1GIP) Structures, As Well As with the MD-Averaged Structure Obtained Using the Last 1 (Solution) and 10 (Vacuum) ns of Trajectory^a

environ-ment	size	temp (K)	rmsd (fiber; Å)	rmsd (X-ray; Å)	rmsd (NMR; Å)	rmsd (MD-av; Å)
water	12-mer	298	2.8 (0.3)	1.8 (0.4)	1.7 (0.3)	1.7 (0.2)
			5.6 (0.5)	6.0 (0.4)	6.3 (0.5)	1.1 (0.3)
gas phase	12-mer	298	7.7 (0.4)	8.0 (0.4)	8.1 (0.4)	1.1 (0.3)
			6.9 (0.4)	7.1 (0.4)	7.4 (0.4)	1.0 (0.3)
water	16-mer	298	7.2 (1.0)	7.4 (1.0)	7.7 (1.0)	1.5 (0.3)
			2.4 (0.5)	10.4 (0.3)	9.7 (0.5)	1.8 (0.5)
gas phase	16-mer	298	10.4 (0.3)	9.7 (0.5)	10.8 (0.7)	1.7 (0.5)
			10.6 (0.7)	10.8 (0.7)	10.6 (0.7)	2.3 (0.8)
gas phase	16-mer	448	10.8 (0.7)	10.6 (0.7)	10.6 (0.7)	2.9 (0.9)
			10.6 (0.7)	10.6 (0.7)	10.6 (0.7)	2.8 (0.6)

^a Standard deviations are in parentheses. Italic numbers correspond to LC (DC) simulations.

as well as the global interaction maps (see Figure 3), are those expected for a canonical B-DNA duplex. Near 71% of the sugars are in the *South* region (around 25% and 4% populate *East* and *North* regions, respectively). Most glycosidic torsions appear in the *anti* region (90%), the remaining 10% being located in the *high-anti* region. Principal component analysis (PCA) shows that the essential motions of the DNA correspond to bending and twisting deformations characterized by frequencies below 20 (12-mer) and 10 cm^{-1} (16-mer), as found in most DNA simulations. In summary, all the analysis confirms the ability of current MD simulation protocols and force fields to reproduce the structure and dynamics of the DNA duplex in aqueous solution.^{25–27}

After 100 ns MD simulation, the structures of the two duplexes in vacuo are very distorted (see Figure 2 and Table 1). The conformational transition due to vaporization is very fast, since after just a few nanoseconds the trajectories seem well equilibrated and sample a relatively narrow region of the conformational space (see Figures 1 and 2 and Table 1). However, the distorted duplexes unexpectedly retain several structural features of its conformation in water, irrespective of the neutralization protocol and the temperature considered. The DNA is found as a very elongated double helix, with packed backbones where the grooves are not clearly defined. The structure in the gas phase is not fully regular, and accordingly does not match any of the standard polymeric structures of DNA determined in solution, fibers, or aqueous solution,^{2,3,28} and some similarities exist with the elongated C-form of DNA.²⁸ Slightly greater similarities exist between the general shape of the DNA in the gas phase and mechanically distorted forms of DNA, such as largely stretched DNAs.^{29,30}

No strand separation was found in any of the trajectories, in agreement with spectroscopic data,^{7–12} suggesting that the two strands remain bound in electrospray experiments. Around 60% of the sugars are in the *South* conformation, 30% in the *East* region, and the rest in the *North* conformation. Nucleotides

(23) Hess, B. *Phys. Rev. E* **2000**, *62*, 8438.

(24) Schlitter, J. *Chem. Phys. Lett.* **1993**, *215*, 617.

(25) Wang, W.; Donini, O.; Reyes, C. M.; Kollman, P. A. *Annu. Rev. Biophys. Biomol. Struct.* **2001**, *30*, 211.

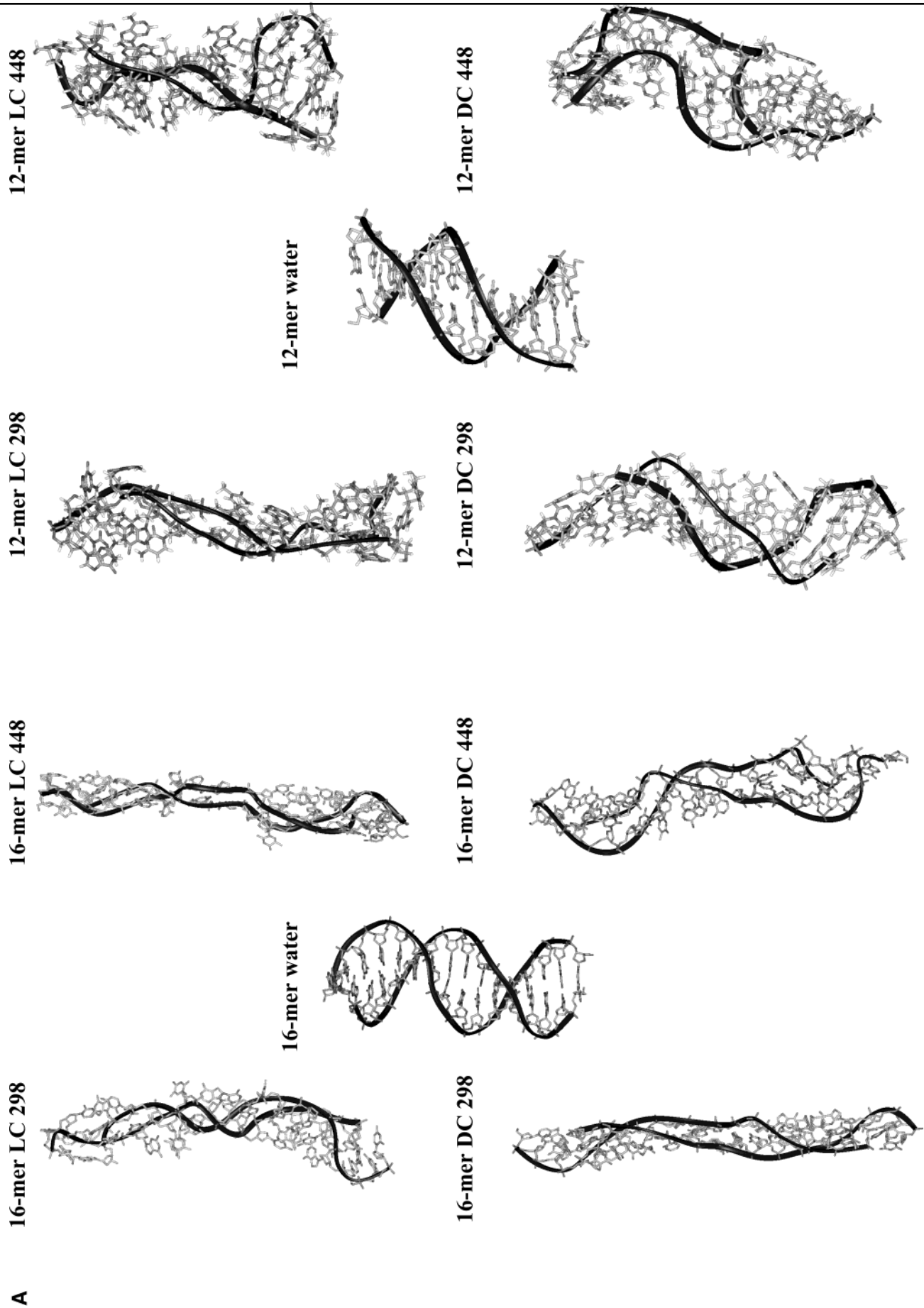
(26) Cheatham, T. E.; Kollman, P. A. *Annu. Rev. Phys. Chem.* **2000**, *51*, 435.

(27) Sprous, D.; Young, M. A.; Beveridge, D. L. *J. Mol. Biol.* **1999**, *285*, 1623.

(28) Saenger, W. *Principles of Nucleic Acid Structure*; Springer-Verlag: New York, 1984.

(29) Kosikov, M. K.; Gorin, A. A.; Zhurkin, V. B.; Olson, W. K. *J. Mol. Biol.* **1999**, *289*, 1301.

(30) Allemand, J. F.; Bensimon, D.; Lavery, R.; Croquette, V. *Proc. Natl. Acad. Sci. U.S.A.* **1998**, *95*, 14152.



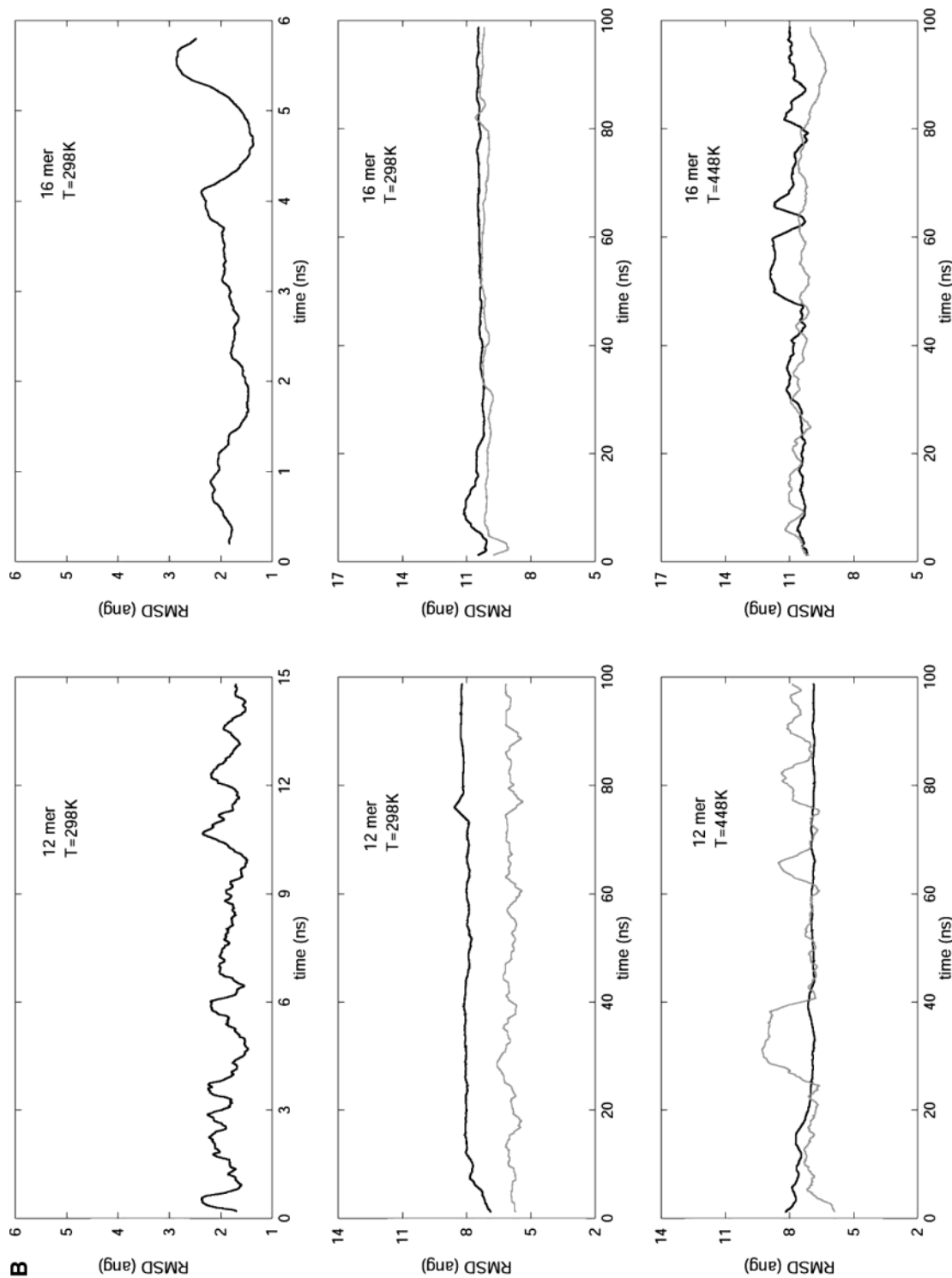


Figure 2. A: MD-averaged structures obtained for the 12-mer and 16-mer duplexes in water and in the gas phase at different temperatures and using different neutralization protocols. Averages were obtained in the 80–90 ns window. B: Root-mean-square deviation (RMSD; Å) between the different trajectories and experimental structures in solution (crystal and fiber data for the 12-mer and 16-mer duplexes, respectively). Dark and light lines correspond to LC and DC simulations, respectively. RMSD with respect to other reference structures are displayed in Table 1.

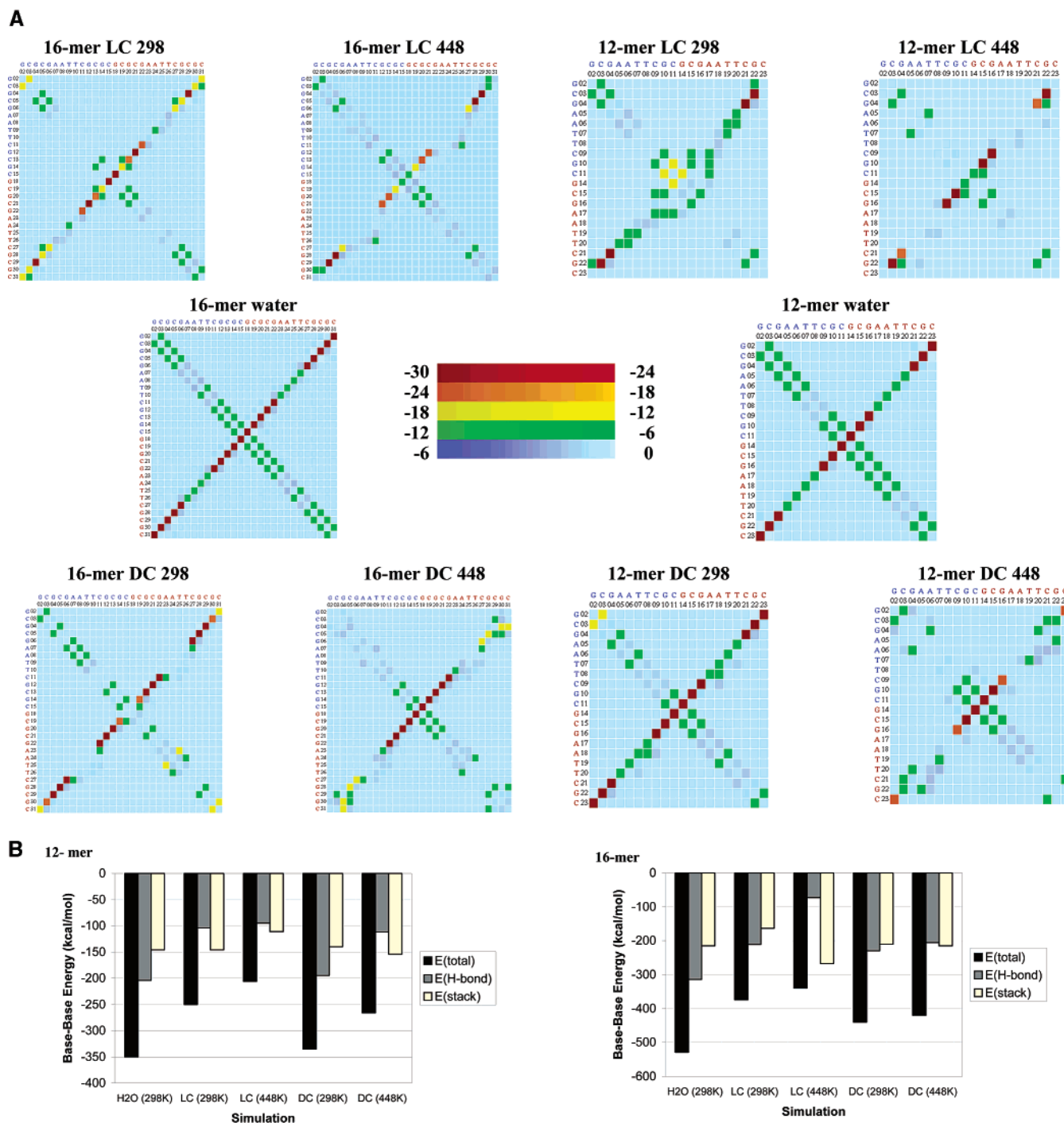


Figure 3. A: Nucleobase–nucleobase interaction maps (kcal/mol) for the 12-mer and 16-mer duplexes in solution and in the gas phase at different temperatures and using different neutralization protocols. Nucleobases were capped at the C1' atom by a CH₃ group to obtain neutral groups. Stacking interactions are shown as $i \rightarrow i + 1$ contacts and H-bond interactions are shown in the $i \rightarrow k + 1 - i$ ($k = 2$ times the oligonucleotide length) diagonal. B: MD-averaged total H-bond and stacking (including both inter- and intrastrand components) interaction energies (kcal/mol) of nucleobases for the 12-mer and 16-mer duplexes in solution and in the gas phase at different temperatures and using different neutralization protocols. A H-bond interaction was accepted if the X...Y distance is less than 3.3 Å and the X–H...Y angle deviates from linearity less than 20°. Two nucleobases are considered to have stacking if they are at less than 3.5 Å and are not H-bonded.

mainly populate the *anti* conformation around the glycosidic bond (84%), with the *high-anti* and *syn* conformations being around 8% each. Therefore, these results reveal that vaporization does not have a dramatic effect on the conformational preferences of nucleotides.

A large number of canonical H-bonds are lost upon vaporization. However, a notable number of H-bonds still exist in the gas-phase DNA (around 30–50% at 448 K and 60–90% at

298 K of the total number of H-bonds found in the aqueous simulations). Most of the canonical H-bonds in vacuo involve G...C pairs, since many canonical A...T pairs are lost at initial stages of the trajectories. Non-canonical H-bonds which are negligible in aqueous solution represent around 20–40% of the total number of H-bonds in the gas phase. The nucleobases are very well stacked during all the simulations but the stacking is not always parallel to the helical axis (see Figure 2). In certain

Table 2. Similarity Indexes γ (Roman) and κ (Italic) and Entropy Values at $t = \infty$ Computed from the Last 10 ns of the Simulations in the Gas Phase of the 12-mer and 16-mer Duplexes^a

	γ/κ similarity indexes					entropy (kcal mol ⁻¹ K ⁻¹)	
	water (298 K)	LC (298 K)	LC (448 K)	DC (298 K)	DC (448 K)	$S_{t=\infty}$	$S_{t=3ns}$
	12-mer						
water (298 K)	1.00/1.00	0.32/0.38	0.30/0.38	0.46/0.54	0.29/0.39	1.9 (0.1)	1.5
LC (298 K)		1.00/1.00	0.26/0.29	0.34/0.35	0.27/0.32	1.9 (0.1)	1.5
LC (448 K)			1.0/1.0	0.31/0.35	0.23/0.30	2.5 (0.2)	1.8
DC (298 K)				1.0/1.0	0.35/0.41	2.0 (0.2)	1.6
DC (448 K)					1.0/1.0	2.8 (0.1)	2.0
	16-mer						
water (298 K)	1.00/1.00	0.26/0.37	0.29/0.44	0.32/0.46	0.31/0.42	3.5 (0.1)	2.8
LC (298 K)		1.00/1.00	0.45/0.56	0.41/0.52	0.32/0.37	3.1 (0.1)	2.6
LC (448 K)			1.0/1.0	0.47/0.66	0.40/0.51	4.7 (0.3)	3.5
DC (298 K)				1.0/1.0	0.49/0.62	3.6 (0.2)	2.7
DC (448 K)					1.0/1.0	5.5 (0.4)	3.7

^a Only the first 10 principal components ($n = 10$ in eq 3), which explain more than 90% of the variance of the trajectory, were considered to compute indexes γ and κ . Comparison between simulations in the gas phase and in water was performed using 3 ns trajectories. For the sake of completeness, entropies were also computed by using the snapshots collected in 3 ns trajectories.

regions nonparallel stacking (T-shaped contacts) is found, involving in some case clusters of three nucleobases (see Figure 2).

The resemblance of the in vacuo DNA to the hydrated duplex is clearly seen in the interaction maps depicted in Figure 3. Favorable interactions are primarily found along the two diagonals of the interaction maps, indicating that the main structural features of the DNA are retained in the gas phase. The H-bond diagonals are quite well preserved in G•••C regions, but disrupted in A•••T regions, thus reflecting the loss of interstrand interactions for A•T pairings upon vaporization (see above). The stacking is also better preserved in G•••C regions, suggesting that the strength of the interactions involving d(G•C) steps is largely responsible for the maintenance of the gross structural features of the DNA upon vaporization. The broadening of the stacking diagonal in A•••T regions found in some simulations suggests that unpaired A–T pairs can establish unusual stacking interactions with other bases. The total base–base interaction energy for simulations in vacuo at 298 K is only 5–29% less favorable than that in aqueous solution, the difference being increased to 25–50% at 448 K (see Figure 3). In general, the DC neutralization scheme leads to better base–base interaction energies, since the reduced phosphate–phosphate repulsion facilitates the formation of a slightly more regular helix. Interestingly, the relative contribution of H-bonding and stacking changes upon vaporization. Thus, the former is 40–50% more intense than stacking in water, but the relative contribution of stacking versus H-bonding increases in the gas phase, specially at high temperature.

All the preceding results point out that the gross geometric and energetic features of the DNA in the gas phase and in water are very similar irrespective of the definition of the model system and the simulation protocol. Furthermore, no dramatic structural changes are found when the temperature is raised to 448 K. Extension of one of the trajectories to 0.25 μ s does not lead to any major change in the structures sampled along the trajectory (see Figure 1), suggesting that the conclusions obtained here are valid in the submicrosecond time scale. In summary, the results strongly support the existence of a well-defined structural deformation pattern of the duplex upon vaporization.

As noted in the Methods section, PCA was used to examine the essential dynamics of the DNA in vacuo. The three principal

modes involve bending and twisting of the DNA and account for more than 60% of the total variance of the trajectories in vacuo. The frequencies of the first modes do not change dramatically with the neutralization scheme nor with temperature, suggesting that the excess kinetic energy between the two temperatures has little impact in the slowest motions of the in vacuo DNA. As expected, the increase in size of the oligonucleotide displaces the first modes to lower frequencies also in the gas phase.

The motion of the 12-mer and 16-mer duplexes involve around 2000 principal components. The overlap between a randomly chosen set of 10 principal components taken from two independent simulations is close to zero (for instance, comparison of the first 10 components of each simulation with 10 random components taken from the same or different trajectories lead to γ values lower than 0.01). Nevertheless, absolute and relative similarity indexes around 0.3–0.5 are obtained between the different trajectories collected in the gas phase (see Table 2), indicating that the essential dynamics of the DNA in vacuo are clearly defined by the nature of the polymer and are not largely affected by either temperature or the neutralization scheme. Similar conclusions can be reached from Schlitter's analysis (see Table 2), which shows that the configurational entropy of the DNA in the gas phase is quite independent of the neutralization scheme, and increases, as expected, when the temperature is raised.

The frequencies associated with the first principal components in the gas phase and in water are not too different, indicating that the extent of the slowest movements of DNA is not dramatically changed upon vaporization. Similarity indexes (see Table 2) reveal a surprising conservation in the nature of the motions which define the essential dynamics of the duplex in the gas phase and in aqueous solution (similarity indexes typically in the range 0.3–0.5). Furthermore, entropy calculations demonstrate that, at the same temperature, the configurational entropy of the DNA duplex in the gas phase and solution is similar (see Table 2). These findings indicate that, though vaporization leads to important structural changes, the DNA in vacuo does not adopt a random coil structure, but it is a rather self-organized duplex that still preserves basic structural, energetic, and dynamic features of the DNA duplex in aqueous solution.

In summary, the analysis of the different MD simulations

points out that the DNA in the gas phase preserves the gross structural, energetic, and dynamic aspects of the DNA duplex in aqueous solution. The results indicate that, under conditions similar to those used in electrospray experiments, vaporization does not lead to separation of the two DNA strands. In fact, they remain tightly bound in MD simulations that cover a total of 1 μ s. The transfer from solution to the gas phase largely distorts the helix, but a reasonable percentage of native nucleobase–nucleobase interactions, specially in G•••C steps, persists along the trajectories. Quite surprisingly, there is also a partial conservation of the type and extent of the principal modes of conformational flexibility of the DNA when trans-

ferred from water to the gas phase. The results, therefore, suggest that the DNA structure in the gas phase retains several structural features of its structure in aqueous solution.

Acknowledgment. We are grateful to Profs. J. Avián, J. L. Gelpí, and E. Giralt for helpful discussions. Computational (IBM Research Center in Barcelona and the Centre de Paral·lelisme CIRI-CEPBA de Barcelona) and financial (Spanish DGCYT; PM99-0046 and PB98-1222) support is acknowledged. M.R. is a predoctoral fellowship of the Spanish Ministry of Science and Technology.

JA0300564